The aza-analogues of 1,4-naphthoquinones are potent substrates and inhibitors of plasmodial thioredoxin and glutathione reductases and of human erythrocyte glutathione reductase†

Christophe Morin,[a] Tatiana Besset,[a] Jean-Claude Moutet,[a] Martine Fayolle,[a] Margit Brückner,[b] Danièle Limosin,[a] Katja Becker[c] and Elisabeth Davioud-Charvet*‡[b,d]

Received 15th February 2008, Accepted 18th April 2008
First published as an Advance Article on the web 30th May 2008
DOI: 10.1039/b802649c

Various aza-analogues of 1,4-naphthoquinone and menadione were prepared and tested as inhibitors and substrates of the plasmodial thioredoxin and glutathione reductases as well as the human glutathione reductase. The replacement of one to two carbons at the phenyl ring of the 1,4-naphthoquinone core by one to two nitrogen atoms led to an increased oxidant character of the molecules in accordance with both the redox potential values and the substrate efficiencies. Compared to the 1,4-naphthoquinone and menadione, the quinoline-5,8-dione **1** and both quinoxaline-5,8-diones **5** and **6** behaved as the most efficient subversive substrates of the three NADPH-dependent disulfide reductases tested. Modulation of these parameters was observed by alkylation of the aza-naphthoquinone core.

Introduction

Tropical malaria is caused by the apicomplexan parasite *Plasmodium falciparum*,[1] which invades and multiplies in red blood cells. Red cell lysis releases fresh merozoites into the blood stream every two days and leads to the fever characterizing malaria. Each year, an estimated number of three million deaths due to malaria and up to 500 million episodes of clinical illness occur worldwide. Africa has more than 90% of this burden.[2] The rapid development of resistance to clinically available drugs leads to the urgent call for the identification of effective and affordable alternative antimalarial regimens.[3–5]

The detoxification of reactive oxygen and nitrogen species (ROS and RNS) is a challenge for erythrocytes infected with *Plasmodium.* Like many tumor cells, malarial parasites grow and multiply rapidly, have a high metabolic rate producing oxidative by-products, are under oxidative attack by the host immune system, and have to detoxify large quantities of redox-active heme.[6] Redox metabolism has thus become an attractive target for antimalarial drug development.[7,8]

The two major antioxidant defense lines in *Plasmodium* are provided by the glutathione and the thioredoxin system.[1,9,10] Both systems are NADPH dependent and are driven by homodimeric FAD-dependent oxido-reductases, namely glutathione reductase (GR, *E.C. 1.8.1.7*) and thioredoxin reductase (TrxR, *E.C. 1.6.4.5*). Glutathione reductase reduces glutathione disulfide into glutathione. Both glutathione reductases from the human erythrocyte and from the malarial parasite were identified as targets of antimalarial drugs.[11,12] Also, Mediterranean populations with genetic glucose-6-phosphate dehydrogenase deficiency provide a natural biomimetic knock-out version of human GR because the enzyme is the main provider of NADPH for GR in the erythrocyte. The deficiency is not lethal for humans but prevents a severe attack of malaria since the oxidative stress released in the red blood cells makes a milieu hostile for *Plasmodium.* Consequently, a rapid elimination of these cells from the circulation occurs by enhanced phagocytosis *via* complement activation.[13] GR is inhibited by numerous redox-cyclers including 1,4-naphthoquinones,[14–16] phenothiazinium derivatives,[17,18] and nitroaromatics.[19] Methylene blue, a potent GR turncoat inhibitor or subversive substrate,[17] was the first synthetic antimalarial drug used in human medicine at the beginning of the 20th century but was abandoned with the launch of chloroquine in the 1940s.[20] Turncoat inhibitors or subversive substrates of disulfide reductases are known to inhibit the physiological reaction while being used as substrates.[21] In the presence of oxygen, the reduced drug is reoxidized following one- or two-electron transfer reactions, leading to both a steady flux of reactive oxygen species and a waste of the NADPH pool in the cells. Hence, the disulfide reductase activity of these antioxidant enzymes is transformed into a prooxidant activity under the efficient catalysis of the subversive substrates. Recently, the GR-catalysed 1,4-naphthoquinone reduction was shown to occur at the flavin of a reduced enzymic species of *Plasmodium falciparum* GR.[16]

TrxR reduces the small protein thioredoxin (Trx) which is present in the parasite in different isoforms involved in redox regulation, peroxidase activity and ribonucleotide reduction.[22] The fact that catalase (detoxifying hydrogen peroxide) and glutathione

[a]*Université Joseph Fourier, Département de Chimie Moléculaire, CNRS UMR-5250, ICMG FR-2607, BP-53, 38041, Grenoble Cedex 9, France*
[b]*Biochemie-Zentrum der Universität Heidelberg, Im Neuenheimer Feld 504, D-69120, Heidelberg, Germany. E-mail: elisabeth.davioud@gmx.de; Fax: +49-6221-54-5586*
[c]*Interdisciplinary Research Center, Justus Liebig University, Heinrich-Buff-Ring 26-32, 35392, Giessen, Germany*
[d]*Centre National de la Recherche Scientifique, Paris, France*

† Electronic supplementary information (ESI) available: ^{1}H and ^{13}C NMR spectra of compounds **1** to **6**. See DOI: 10.1039/b802649c

‡ Delegate (E.D.C.) of Centre National de la Recherche Scientifique, France in the frame of a French–German cooperation with Heidelberg University, Germany.

peroxidase (reducing peroxides glutathione-dependently) are absent in the parasite suggests that the thioredoxin system plays a prominent role in *P. falciparum*. This hypothesis is supported by PfTrxR knock-out studies, proving that this enzyme is essential for erythrocytic stages of the parasite.[23] In comparison with GR, TrxR possesses an additional redox center which is located on a flexible C-terminal arm. PfTrxR has been mechanistically studied in detail including the different steps of electron transfer and the function of the active site residues.[10,24,25] The fact that PfTrxR is not selenium-dependent and differs in its C-terminal active site motif (CGGGKC) from human TrxR (Cys-Sec) represents a specific starting point for the development of antiparasitic drugs. Several lines of drug development are presently being followed.[7,10,24,26] A high-throughput screening of 350 000 compounds identified Mannich bases[27,28] and nitroaromatics[29] as new classes of TrxR mechanism-based inhibitors or subversive substrates. Optimization of subversive substrates as catalytic inhibitors is a promising strategy to catalytically affect the reducing milieu of target cells and to observe specific cell responses. In order to increase the rate of the electron bypass at the reduced flavin of disulfide reductases, the design of new 1,4-naphthoquinones with increased oxidant character and affinity is essential.

Among all synthetic 1,4-naphthoquinones developed as antimalarial drugs so far, only atovaquone was launched on the market. Hydroxy-naphthoquinones are competitive inhibitors of the cytochrome bc_1 complex that bind to the ubiquinol oxidation site between cytochrome b and the iron–sulfur protein and presumably mimic a transition state in the ubiquinol oxidation reaction catalyzed by the enzyme.[30] As mentioned earlier,[31] only quinones, *e.g.* menadione, of the appropriate redox potentials are likely to be toxic to red cells by affecting the redox equilibrium. Atovaquone, which has a higher redox potential, has no effect on disulfide reductases (data not shown). To optimize the antimalarial hydroxy-naphthoquinones, some hydroxy-5,8-quinolinediones were also synthesized as atovaquone analogues.[32] Also, a direct link had been earlier evidenced between the selective guanylate cyclase inhibitor 6-anilino-5,8-quinolinedione (LY83583) and the GSSG increase resulting from GR-catalysed reduction of the compound, but no optimization based on structure–GR inhibition relationships was further developed.[33]

Here, we describe the aza-analogues of 1,4-naphthoquinones as potent substrates and inhibitors of disulfide reductases, particularly of *P. falciparum* TrxR. The reactivity of quinoline-5,8-diones and quinoxaline-5,8-diones was compared to that of 1,4-naphthoquinones to examine the effect of nitrogen of the heterocycle on redox potentials, and both inhibitory capabilities and substrate efficiencies in three disulfide reductase assays.

Results and discussion

Chemistry

Quinolinediones and quinoxalinediones **1–6** are described compounds, and known approaches for the chemical preparations were applied here with slight modifications and by taking into account the availability of the starting materials (Scheme 1). For example, quinolinedione **1** can be derived from the commercially available 8-hydroxyquinoline following oxidation with potassium nitrosodisulfonate[34,35] or with oxygen,[36,37] but we found

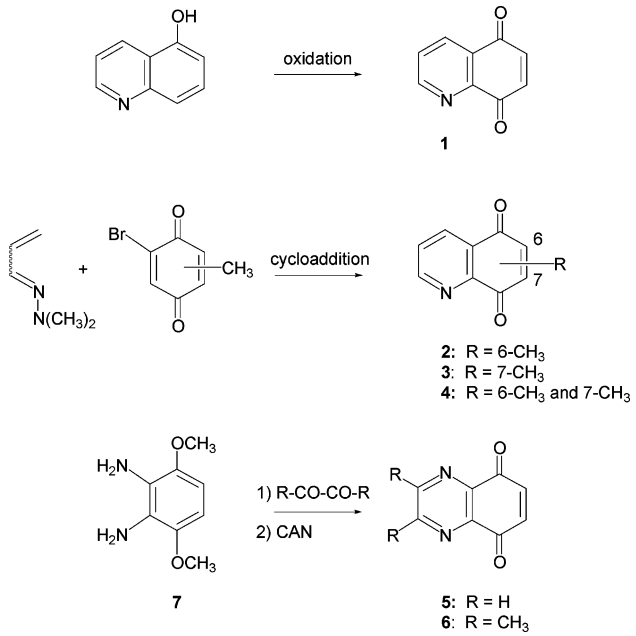

Scheme 1 Routes to 5,8-quinolinediones and 5,8-quinoxalinediones.

it more convenient to use bis(trifluoroacetoxy)iodobenzene as the oxidizing reagent.[38] The methyl-substituted analogues, **2**,[39] **3**,[40,41] and **4**,[42] which were previously prepared from oxidation of aminoquinoline derivatives, were obtained here by cycloadditions of an 1-azadiene[43] with bromo-quinone partners; indeed, although 1-azadienes are not that reactive—for a discussion of relevant factors see ref. 44—the cycloaddition of acroleine-*N,N*-dimethylhydrazone[45] proceeded with 5-methyl-,[46,47] 6-methyl,[48,49] and 5,6-dimethyl-[50] 2-bromobenzoquinones to produce the desired quinones (**2** and **3** < 10%; **4**, 40%).

Quinoxalinediones **5**[51,52] and **6**[51,52] could be obtained *via* a Hinsberg reaction of *ortho*-diamine **7** with glyoxal or biacetyl respectively, which was followed by ceric ammonium nitrate (CAN) oxidation (Scheme 1). While several procedures have been recently devised to ease the isolation of diamine **7** in the pure state[51,53,54] from the reduction of a mixture of *ortho* and *para* dinitro isomers (**8**/**9**) (Scheme 2), it was found advantageous to perform

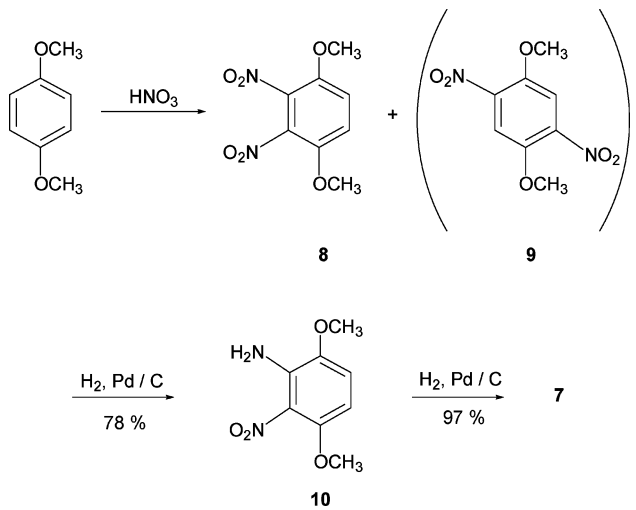

Scheme 2 Obtention of *ortho*-diamine **7**.

a step-by-step reduction[55] since the *ortho* amino nitro **10** could be easily isolated in good yield by mere filtration on a short column of silica gel; such a stepwise procedure avoids the separation of **8** and **9** or of the corresponding diamines (it is noteworthy to mention that the preparation of the synthetically-useful building-block **10**[56,57] previously derived in 5 steps from 2,5-dihydroxybenzoic acid[58] is here significantly improved). Then, condensation of **7** with glyoxal or diacetyl followed by CAN oxidation (Scheme 1) afforded **5** and **6** in pure state (68% and 85% overall yield, respectively).

Electrochemistry

The reduction of aza-analogues of 1,4-naphthoquinone and menadione has been studied using cyclic voltammetry in organic and aqueous electrolytes. In agreement with a previous study,[59] it appears that the quinoline-5,8-dione is easier to reduce to its radical anion form than the 1,4-naphthoquinone, ($E_{1/2} = -0.57$ and -0.66 *versus* SCE in DMF electrolyte, respectively). It is also known that the quinoxaline-5,8-dione is reduced at a more positive potential than the 5,8-quinolinedione in organic electrolytes.[59] In addition, $E_{1/2}$ values for the reversible one-electron reduction of quinolinediones, recorded in DMF as solvent, provide data on their relative ease of reduction according to the substitution by methyl groups at the 6 and 7 positions. The reduction potential for the quinoline-5,8-dione ($E_{1/2} = -0.57$ *versus* SCE) is in good agreement with that already found in the same electrolyte ($E_{1/2} = -0.62$ *versus* Ag/AgCl).[59] Not surprisingly, the quinolinediones are increasingly difficult to reduce when they are substituted with one ($E_{1/2} = -0.63$ to -0.64 V *versus* SCE) and two ($E_{1/2} = -0.72$ *versus* SCE) electron-donating methyl groups. Little variation of the $E_{1/2}$ value ($\Delta E = 10$ mV) is observed when the aza-naphthoquinone is substituted with a methyl group at the 7 position instead of at the 6 position.

It is well known that reduction of quinones in aqueous electrolytes consumes two electrons and two protons to form the corresponding hydroquinones and that the reduction potential is pH-dependent.[60] It has been established that the quinolinediones present a similar reduction behavior.[61] For the quinoxalinediones, the reduction occurs in a two-step process since the reduction of the quinone moiety is followed at a more negative potential than the value observed for the reduction of the quinoxaline moiety.[62] The reduction of 1,4-naphthoquinone, menadione, and different aza-analogues of naphthoquinone has been studied under physiological conditions in phosphate buffer at pH 7. The cyclic voltammetry data are summarized in Table 1. The reduction peak potential values follow the same trends as the half-wave potentials measured in organic electrolytes. As a matter of fact, the absence of an electron-donating methyl group in the 1,4-naphthoquinone makes it easier to reduce than the menadione. Moreover, the mono-substituted quinoline-5,8-diones **2** and **3**, at the 6 or 7 positions by methyl groups, are easier to reduce than menadione itself; the absence of an electron-donating methyl group in the quinolinedione **1** makes it much easier to reduce but the presence of two methyl groups in the di-substituted quinoline-5,8-dione **4** affects the redox potential to more negative values. As expected, the quinoxalinedione **5** presents the more oxidant character, while its 2,3-dimethyl derivative **6** appears slightly more difficult to reduce. A similar trend was observed for the reduction of aza-anthraquinones in DMF, where the 1,4,5,6-tetraazaanthra-9,10-quinone appeared easier to reduce than its 2,3,6,7-tetramethyl derivative.[59] Noteworthy is that recent studies on humanNAD(P)H:quinone oxidoreductase, identified as a two-electron reductase upregulated in tumour cells, was shown to be inhibited by heterocyclic quinones with increased oxidant character and acting as excellent substrates of this flavoenzyme.[63,64]

Table 1 Cyclic voltammetry data[a] for reduction of the quinones[b] in phosphate buffer (pH 7)

Quinone	Structure	E_{pc} (V *versus* SCE)	E_{pc} (V *versus* $MV^{2+}/MV^{\bullet+}$)[c]
1,4-NQ	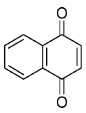	−259	0.464
Menadione	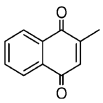	−0.335	0.388
1	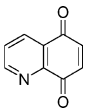	−0.218	0.505
2	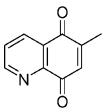	−0.279	0.444
3	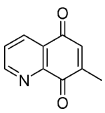	−0.282	0.441
4	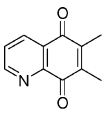	−0.317	0.406
5	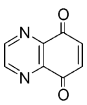	−0.163	0.560
6	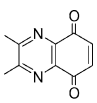	−0.211	0.512

[a] E_{pc} is the reduction peak potential; scan rate 100 mV s^{-1}. [b] Potential of the quinone/hydroquinone redox system. [c] Measured *versus* the $MV/MV^{\bullet+}$ redox couple used as an internal reference. Under the same conditions, methylene blue, plumbagin, and naphthazarin exhibited reduction potential values of −0.23 and 0.49, −0.320 and 0.403, and −0.330 and 0.393, respectively.

Enzyme studies

Inhibition of human and *P. falciparum* glutathione reductases (hGR, PfGR) and *P. falciparum* thioredoxin reductase (PfTrxR) by the aza-naphthoquinones was followed under steady-state conditions. As previously observed,[16] inhibition of disulfide reductases depends on both the redox potentials and the structural features

governing recognition by the enzyme. Following the determination of the redox potentials of the mono- and diaza-naphthoquinones by cyclic voltammetry, we evaluated the influence of the nitrogen atom(s) at the naphthoquinone core on the inhibitory potencies. In all enzyme assays, the activity was directly measured in the presence of different concentrations of the inhibitor at a fixed substrate concentration (1 mM GSSG and 26 μM $Trx(S)_2$ in GR and TrxR assays, respectively). The inhibitor concentrations causing 50% inhibition are given in Table 2 and compared to the values of menadione and 1,4-naphthoquinone (**1,4-NQ**). In GR assays, as previously discussed, the high GSSG concentration is used in order to select the most effective inhibitors (IC_{50} values $\leq$ 10 μM) by comparison with menadione (IC_{50} values = 42 μM and 27.5 μM in PfGR and hGR assays, respectively) and 1,4-naphthoquinone (IC_{50} values = 2.2 μM and 1.3 μM in PfGR and hGR assays, respectively). In TrxR assays, low IC_{50} values for menadione and 1,4-naphthoquinone were obtained (IC_{50} values = 1.6 and 0.75 μM, respectively). Under these conditions, all three FAD-disulfide oxidoreductases are inhibited by aza-naphthoquinones with different specificities. While the 1,4-naphthoquinone is the most potent inhibitor of all disulfide reductases, the quinolinedione **1**, and both quinoxalinediones **5** and **6**, behaved as the most specific TrxR inhibitors with a similar (even slightly increased) inhibition profile as shown by menadione. Among the three aza-analogues, the quinoxalinedione **5** is as active as the 1,4-naphthoquinone (IC_{50} values = 0.8 μM). The three compounds are poor GR inhibitors with IC_{50} values higher or in the same range as the values shown by menadione. Regarding the GR assays, the aza-analogue of menadione, the quinolinedione **2**, is the most potent GR inhibitor with the lowest IC_{50} values determined in this study.

Table 2 Aza-analogues of menadione as inhibitors of *P. falciparum* and human glutathione reductases and of *P. falciparum* thioredoxin reductase

Quinone	Structure	IC_{50} /μM		
		PfTrxR	PfGR	hGR
1	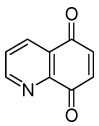	1	>130	>150
2	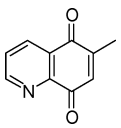	3	11	9
3	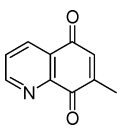	16	28	13
4	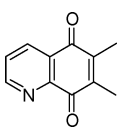	10	25	18
5	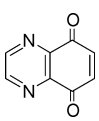	0.8	37	36
6[a]	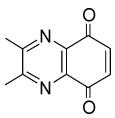	1	85	34
Menadione	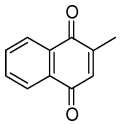	1.6	42[b]	27.5[b]
1,4-NQ	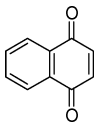	0.75	2.2	1.3

[a] Reacts with NADPH at high concentration. [b] From ref. 16

In order to investigate the inhibition of *P. falciparum* TrxR at varying Trx concentrations (6–244 μM), kinetics were performed with saturating NADPH (100 μM) and GSSG (1 mM) concentrations in the presence of potent (aza)-naphthoquinones, **1,4-NQ** (Fig. 1, panels A,B) or **6** (Fig. 1, panels C,D). Both Cornish–Bowden plots (panels A,C, Fig. 1) and Lineweaver–Burk plots (panels B,D, Fig. 1) for **1,4-NQ** and **6** were consistent with competitive inhibition (eqn (1) in the experimental part). From secondary plots (insets from panels B,D) expressing $1 + [I]/K_i$ as a linear function of inhibitor concentration, the K_i values for **1,4-NQ** and **6** were determined as 0.20 ± 0.01 μM and 0.49 ± 0.02 μM, respectively. This result is similar to the recent determination of the inhibition type found for 9,10-phenanthrene quinone and rat TrxR.[65] Using DTNB as the disulfide substrate, 9,10-phenanthrene quinone was found to be competitive with a K_i value of 6.3 μM.

In the assays in the absence of the physiological disulfide, the enzyme-catalysed quinone reductase activity was determined following NADPH oxidation at varying quinone concentrations. The same three aza-naphthoquinones, the quinolinedione **1**, and both quinoxalinediones **5** and **6**, behaved as the most efficient TrxR substrates with catalytic efficiencies, as shown by the k_{cat}/K_m values (Table 3), higher than those of menadione. This observation is in agreement with the higher oxidant character of these compounds revealed by cyclic voltammetry. In the GR assays, the quinolinedione **1** and the quinoxalinedione **5** displayed the greatest efficiencies when compared with menadione. Surprisingly, the three aza-analogues of menadione, **2**, **3**, and **4**, showed decreased dynamic specificities, evidencing that the redox potential is not the sole requirement to divert the electrons at the reduced enzyme. Structural features are likely to play a role in GR recognition. Most of the quinones studied in this work showed classical Michaelis–Menten kinetics in agreement with the various plots shown in Fig. 2. In some enzymic studies, sigmoidal responses were observed showing the complexity of the kinetics in the presence of compounds **3**, **4**, and **6** (noted as 'nd' in Table 3).

The $FADH_2$-mediated quinone reduction has been evidenced with GR, and other related disulfide reductases.[65] Since in TrxR the reducing equivalents are transferred from NADPH *via* FAD to the N-terminal active site and from there to the C-terminal active site of the other subunit, the active site thiol (selenol) residues were also suggested to be involved in the mechanism of inactivation

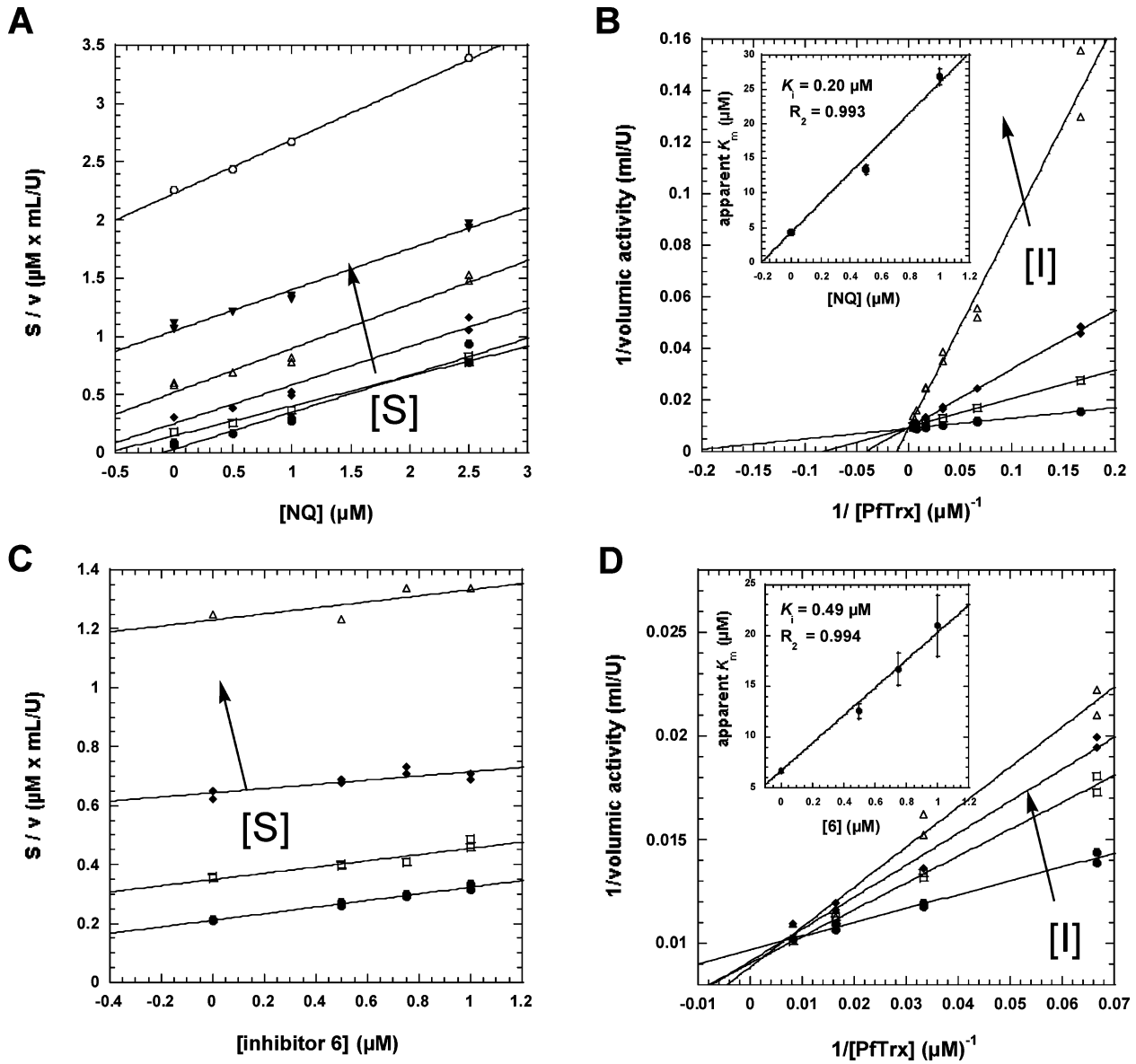

Fig. 1 Inhibition of *P. falciparum* thioredoxin reductase by 1,4-naphthoquinone (**1**,**4-NQ**) and the aza-naphthoquinone **6** under steady-state conditions. Panels A,C: Cornish–Bowden plots showing inhibition of PfTrx reduction at a fixed NADPH concentration (100 µM) in the presence of 1mM GSSG and PfTrx as variable substrate, and increasing inhibitor concentrations: 0–0.5–1.0–2.5 µM **1**,**4-NQ** (panels A,B) and 0–0.5–0.75–1.0 µM inhibitor **6** (panels C,D). Trx concentrations used were 6 (●) – 15 (□) – 30 (♦) – 61 (△) – 122 (▼) – 244 (○) µM in the experiment with **1**,**4-NQ** (panels A,B); in the experiment with **6** Trx concentrations used were 15 (●) – 30 (□) – 61 (♦) – 122 (△) µM (panels C,D). 1% final DMSO was present in all measurements. Panels B,D: corresponding Lineweaver–Burk plots showing inhibition of PfTrx reduction using the same PfTrx, GSSG, NADPH and inhibitor concentrations as given in panels A,C, respectively. Insets from panels B,D: secondary plots expressing $1 + [I]/K_i$ as a linear function of inhibitor concentration for **1**,**4-NQ**, inset panel B and for **6**, inset panel D. Assuming competitive inhibition with respect to PfTrx, the K_i values for **1**,**4-NQ** and **6** were determined as 0.20 ± 0.01 µM and 0.49 ± 0.02 µM, respectively.

by naphthoquinones. As previously described by Cenas *et al.*,[65] various quinones are reduced efficiently by TrxR. Certain quinones (*e.g.* phenanthrene-9,10-quinone) were proposed to be mainly reduced by the C-terminal selenol thiol motifs of mammalian TrxR whereas other quinones (*e.g.* juglone) are reduced at the N-terminal active site in interaction with the enzyme-bound FAD.

Finally, inactivation of *P. falciparum* TrxR by two representatives, *i.e.* **1**,**4-NQ** and **5**, among the most potent naphthoquinones is shown, and it followed pseudo-first order reaction kinetics. The experimental data allowed us to apply the derivation established by Kitz and Wilson[66] for irreversible inactivation. Semi-logarithmic plots (Fig. 3, panels A,B) of the fraction of non-inhibited enzyme activity $\ln(v_i/v_0)$ *versus* incubation time yielded linear curves with increasing slopes, equivalent to the apparent rate constant of irreversible inhibition (k_{obs}). The secondary plot (Fig. 3, insets of panels A,B) expressing k_{obs} as a function of inhibitor concentration followed eqn (2) given in the experimental part, where K_I represents the dissociation constant of the inhibitor, and k_i is the first order rate constant for irreversible inactivation, respectively. The dose-response curve for **1**,**4-NQ** and the *P. falciparum* TrxR,

Table 3 Kinetic parameters of *P. falciparum* thioredoxin and glutathione reductases, and of human glutathione reductase with the aza-naphthoquinone analogues as substrates

	Kinetic parameters								
	PfTrxR			PfGR			hGR		
Quinone	K_m/μM	k_{cat}/s^{-1}	k_{cat}/K_m/10^3 M^{-1} s^{-1}	K_m/μM	k_{cat}/s^{-1}	k_{cat}/K_m/10^3 M^{-1} s^{-1}	K_m/μM	k_{cat}/s^{-1}	k_{cat}/K_m/10^3 M^{-1} s^{-1}
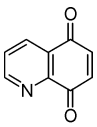 **1**	78.3	30.25	386.3	234.4	1.55	6.61	363.5	2.23	6.13
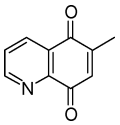 **2**	605.4	67.35	111.2	410.4	0.35	0.83	420.8	0.35	0.83
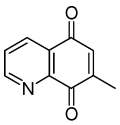 **3**	nd	nd	nd	404.4	0.39	0.96	224.5	0.13	0.58
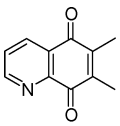 **4**	nd	nd	nd	85.8	0.08	0.99	413.0	0.11	0.27
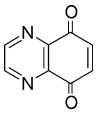 **5**	28.6	6.25	218.3	56.2	0.35	6.2	59.5	0.34	5.71
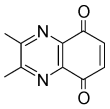 **6**	51.0	9.23	181.0	nd	nd	nd	nd	nd	nd
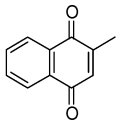 **menadione**	188.0	30.7	163.5	82.2	0.16	1.99[a]	31.2	0.16	5.33[a]
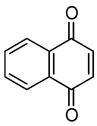 **1,4-NQ**	69.4	12.5	180.1	172.1	1.08	6.3	158.1	1.08	6.8

[a] From ref. 15; nd: not determined.

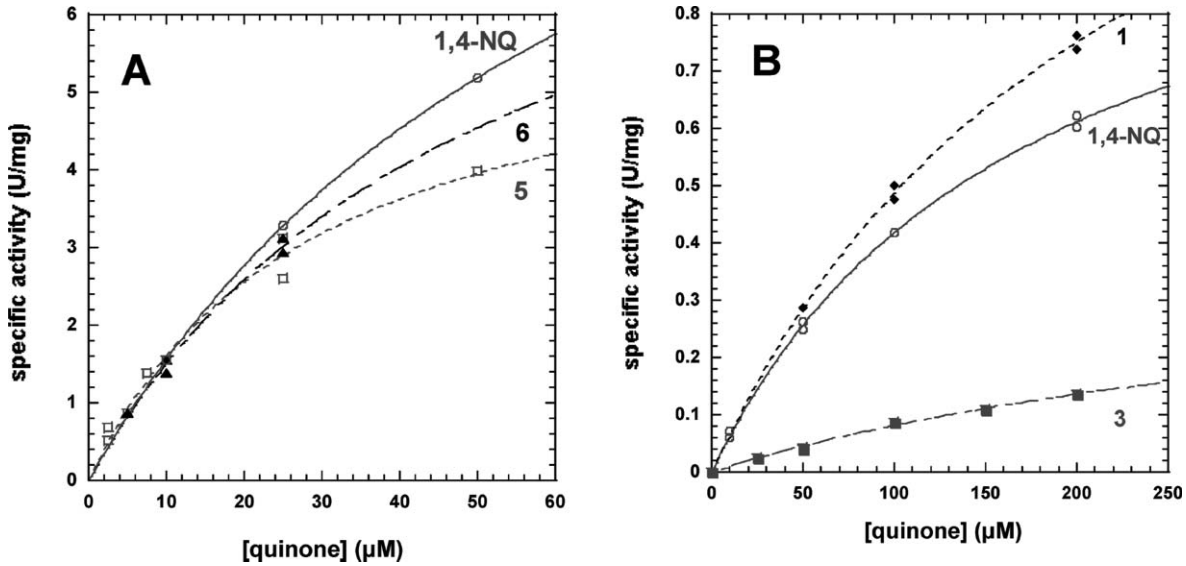

Fig. 2 Quinone reductase activity of thioredoxin and glutathione reductases from *P. falciparum.* The quinone reductase activity of *P. falciparum* TrxR (panel A) in the presence of 1,4-naphthoquinone (**1,4-NQ**) (–○–), or **5** (–□–), or **6** (–▲–), and of *P. falciparum* GR (panel B) in the presence of **1**,**4-NQ** (–○–), or **1** (–◆–), or **3** (–■–) was tested by monitoring the oxidation of NADPH at 340 nm, at 25 °C, and pH 7.4 in TrxR assay (pH 6.9 in GR assays), under steady-state conditions. The quinone was dissolved in DMSO and the NADPH-oxidation activity was measured at four to five different concentrations in duplicate (0–200 μM) in the presence of 1% DMSO. The initial rate for aerobic NADPH oxidation activity of modified *P. falciparum* enzymes was subtracted from the rates measured in the presence of the naphthoquinone. For the determination of K_m and V_{max} values, the steady-state rates were fitted by using nonlinear regression analysis software (Kaleidagraph) to the Michaelis–Menten equation,[75] and the turnover number k_{cat} and the catalytic efficiency k_{cat}/K_m were calculated.

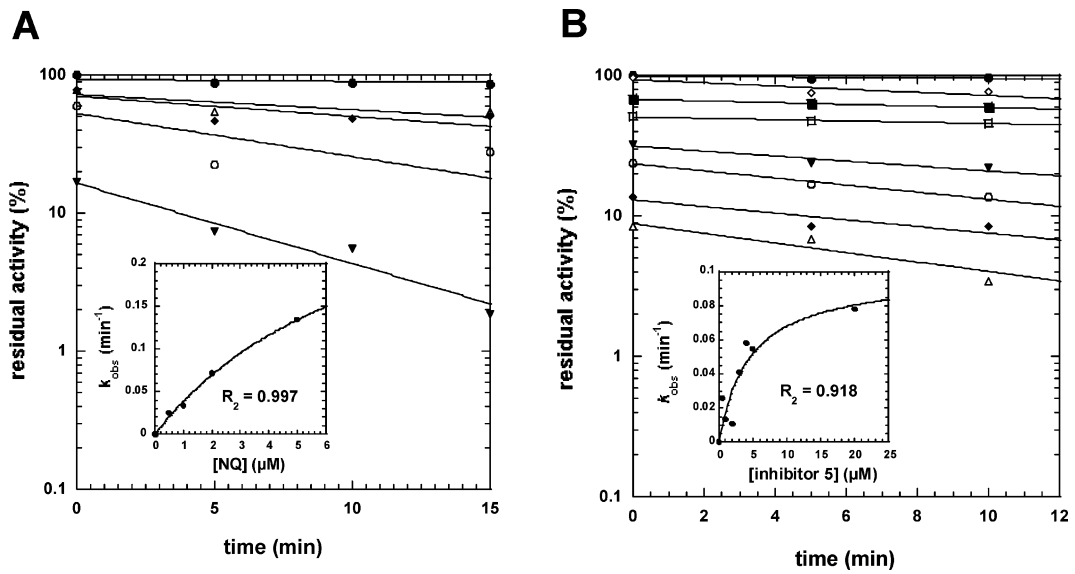

Fig. 3 Time-dependent inactivation of *Plasmodium falciparum* thioredoxin reductase by 1,4-naphthoquinone (**1**,**4-NQ**) and the aza-naphthoquinone **5**. *P. falciparum* TrxR (1.23 nmol in 200 μL) was incubated in the presence of 160 μM NADPH and inhibitor at 0.25, 5, 10, and 15 min-incubation periods. 2% final DMSO was present in all incubation mixtures. Inhibitor concentrations used were: 0 (●), 0.5 (△), 1.0 (◆), 2.0 (○), and 5.0 (▼) μM for **1**,**4-NQ** (panel A) and 0 (●), 0.5 (◇), 1.0 (■), 2.0 (□), 3.0 (▼), 4.0 (○), and 5.0 (◆) for aza-naphthoquinone **5** (panel B). The k_{obs} data *versus* [I] were fitted to eqn (2) (see text), which resulted in the hyperbolic curve shown in the inset from both panels A and B. The dissociation constants and the first order rate constants for irreversible inactivation for **1**,**4-NQ** (inset, panel A) and aza-naphthoquinone **5** (inset, panel B), were determined as $K_I = 8.0 \pm 2.2$ μM and $k_i = 0.35 \pm 0.06$ min^{-1} and $K_I = 4.4 \pm 2.2$ μM and $k_i = 0.10 \pm 0.02$ min^{-1}, respectively.

gave a hyperbolic curve, allowing estimation of k_i as 0.35 ± 0.06 min^{-1}, $K_I = 8.0 \pm 2.2$ μM, and second order rate constant k_i/K_I as 0.7×10^3 M^{-1} s^{-1} (Fig. 3, inset of panel A). The resulting half-time value ($t_{1/2}$) of inactivation of *P. falciparum* TrxR was determined as 2.0 min. In an additional kinetic experiment (Fig. 3, panel B), we observed that *Plasmodium* TrxR was also inactivated upon incubation of the enzymes with NADPH and the aza-naphthoquinone **5**. The rate constant k_i, the dissociation constant K_I, the second order rate constant k_i/K_I of the inhibitor **5** and the resulting half-time value ($t_{1/2}$) for the inactivation of *P. falciparum*

TrxR were determined as 0.10 ± 0.02 min^{-1}, 4.4 ± 2.2 μM, 0.4×10^3 M^{-1} s^{-1}, and 7.0 min, respectively (Fig. 3, inset of panel B). In both cases, incubation of the enzymes with inhibitor in the absence of NADPH did not result in any inactivation, indicating that reduction of the enzyme is a prerequisite for this mechanism-based inactivation.

Furthermore, the inactivation of *P. falciparum* TrxR studied in this work was compared with other studies performed with rat TrxR.[65] For rat TrxR inactivation, a prereduction of the enzyme was also necessary. Interestingly, in this study, the fully substituted aziridinylbenzoquinones and daunorubicin, which are used as anticancer agents, were poor substrates and almost inactive as reversible inhibitors of rat TrxR ($K_i \geq 400$ μM in the DTNB assay) but were able to inactivate the enzyme significantly, suggesting no correlation between disulfide reduction, substrate efficiencies, and enzyme inactivation. This lack of correlation was also observed with trypanothione reductase inhibitors by us and other groups. The most rational explanation might involve cooperative effects towards the binding of NADPH and oxidant molecules (*e.g.* O_2, quinones) responsible for complex kinetics with the different members of the NADPH-dependent disulfide reductases. In our study, the non Michaelis–Menten behaviour was also observed in quinone reduction assays with some aza-naphthoquinones that showed sigmoidal responses when the initial velocity was plotted as a function of the quinone concentration (data not shown). Thus, the type-dependent inhibition of flavoenzymes by electron-acceptors might not necessarily imply irreversible covalent modification of the protein. This hypothesis is supported by previous studies involving alkylated quinones—where Michael addition by nucleophiles is not possible—showing a high rate of rat TrxR inactivation despite a weak competitive inhibition under steady-state conditions.[65] The TrxR inactivation observed by us and other groups could be interpreted as the result of the shift of the equilibrium between distinct reduced enzymic species involved in the catalytic cycle in favour of the generation of an inactive enzyme in the presence of an excess of both NADPH and quinones or O_2. In the future, more work is necessary, likely under anaerobic conditions, in the field of single-enzyme kinetics based on confocal microscopy techniques, and photoaffinity labeling studies along with mass spectrometry analyses.

In conclusion, our results show that the modulation of disulfide reduction inhibition by 1,4-naphthoquinones can be achieved both by the introduction of nitrogen atoms within the aromatic ring as well as by variation of the substitution pattern of the naphthoquinone core. In the future, introduction of the structural diversity at the quinoline-5,8-dione and quinoxalin-5,8-dione might render possible the selection of specific lead compounds to develop as antimalarial agents through the plasmodial TrxR and GR inhibition.

Experimental

Chemistry

All starting chemicals, including the studied 1,4-naphthoquinone, menadione, plumbagin, and methylene blue, were purchased from Acros or Aldrich and used as received. Reactions were monitored by thin layer chromatography (TLC) using aluminium-backed silica gel plates (Merck, Kieselgel 60 PF_{254}); TLC spots were visualized under ultraviolet light and also after spraying with 5% ethanolic phosphomolybdic acid followed by heating. Chromatographic purifications were performed by column chromatography using Macherey-Nagel silica gel 60 (0.063–0.2 μm). Melting points were recorded (heating rate = 1° C min^{-1}) on a Büchi B-545 apparatus. IR spectra were recorded with a Nicolet 'Magna 550' spectrometer using ATR (attenuated total reflexion). NMR spectra were recorded on Bruker Advance 300.12 or Advance 400.13 spectrometers; chemical shifts (δ) are given in ppm using internal reference (δ [^{1}H] C*H*Cl$_3$ = 7.26, δ [^{13}C] *C*DCl$_3$ = 77.0); coupling constants, *J*, are given in Hertz. Mass spectra were obtained with a Bruker Daltonics Esquire 3000 Plus ion-trap spectrometer (ESI) and with a Thermo Fisher Scientific Polaris Q spectrometer, using ammonia–isobutane 63 : 37 for chemical ionisation. Elemental analyses were performed by the 'Service de Micro-Analyses', Département de Chimie Moléculaire, Grenoble.

Quinoline-5,8-dione 1

To a solution of bis(trifluoroacetoxy)iodobenzene (2.500 g, 2.30 mmol, 1.15 equiv.) in acetonitrile (4 mL) was added water (2 mL); after cooling to 4 °C (which resulted in some precipitation), 8-hydroxyquinoline (0.290 g, 2.0 mmol) was added portionwise and the cooling bath was removed; the resulting mixture was then stirred for 3 h (the reaction was stopped after all starting material had been consumed, thus allowing isolation of **1** without chromatography). After filtration of the insoluble fraction, water (10 mL) was added and acetonitrile evaporated under reduced pressure; the aqueous layer was extracted with dichloromethane and the organic layer thoroughly washed with water to yield, after drying and evaporation of the volatiles, **1** (0.283 g, 89%); mp 105 °C (dec.) from EtOH (lit.,[40] 113–5 °C); (Found: C, 67.96; H, 3.21; N, 8.69. Calc. for $C_9H_5NO_2$: C, 67.93; H, 3.17; N, 8.81%); λ_{max} (EtOH/nm) 240.1 (lit.[40]); ν_{max}(neat)/cm^{-1} 2970 (C–H), 1668 (C=O) and 1578 (C=C); δ_H(300 MHz; $CDCl_3$) 7.05 (2H, AB system, *J* 10.3, 6-H/7-H), 7.64 (1H, dd, *J* 8.0 and 4.7, 3-H), 8.37 (1H, dd, *J* 8.0 and 1.7, 4-H) and 9.00 (1H, dd, *J* 4.7 and 1.7, 2-H), (lit., ref.[66]); δ_C (75 MHz; $CDCl_3$) 127.8, 129.1, 134.5, 138.0, 139.1, 147.4, 154.8, 183.1 (C=O) and 184.5 (C=O), (lit., ref.[67]); *m*/*z* (DCI$^+$) 160.1 ([M + H]$^+$).

2-Bromo-5-methyl-1,4-benzoquinone

To a stirred solution of 4-bromo-2,5-dimethoxytoluene[68] (0.300 g, 1.30 mmol) in acetonitrile (6 mL) was added dropwise a solution of ceric ammonium nitrate (2.139 g, 2.90 mmol, 3 equiv.) in water (6 mL). After 30 minutes at room temperature, the mixture was extracted with $CHCl_3$ (3 × 10 mL) and the organic layer was washed with water (10 mL), dried over $MgSO_4$ and concentrated to afford the title compound (0.237 g, 1.18 mmol, 91%); mp 94–5 °C (lit.,[47] 105–7 °C); (Found: C, 41.91; H, 2.19. Calc. for $C_7H_5BrO_2$: C, 41.83; H, 2.51%); ν_{max}(neat)/cm^{-1} 3039 (CH_3), 1646 (C=O), 1626 (C=O), 1585 (C=C) and 670 (C–Br); δ_H(400 MHz; $CDCl_3$) 2.07 (3H, d, *J* 1.5, CH_3), 6.79 (1H, q, *J* 1.5, 6-H) and 7.27 (1H, s, 3-H), (lit., ref.[49]); δ_C(100 MHz; $CDCl_3$) 15.6 (CH_3), 132.5 (CH), 137.4 (C_{quat}), 138.1 (CH), 146.4 (C_{quat}), 179.4 (C=O) and 185.1 (C=O), (lit., ref.[49]); *m*/*z* (DCI$^-$) 200.3 and 202.2 ([M]$^-$).

6-Methylquinoline-5,8-dione 2

To a solution of 2-bromo-5-methyl-1,4-benzoquinone (60 mg, 0.297 mmol) in toluene (2 mL) was added acrolein dimethylhydrazone[45] (30 mg, 0.297 mmol, 1 equiv.). The reaction mixture was heated at 80 °C for 4 h, and after cooling and evaporation of the volatiles, the crude residue (83 mg) was purified by chromatography on silica gel (ether with gradient of ethanol) to give **2** (5 mg, 9%); mp 141 °C (dec.), (lit.,[40] 177–80 °C (dec)); λ_{max} (EtOH/nm) 260.0, 240.1 (lit.[40]); ν_{max}(neat)/cm^{-1} 3061 (CH_3), 2924 (C–H), 1676 (C=O), 1660 (C=O) and 1575 (C=C); δ_H(300 MHz; $CDCl_3$) 2.27 (3H, d, *J* 1.5, CH_3), 6.92 (1H, q, *J* 1.5, 7-H), 7.66 (1H, dd, *J* 7.8 and 4.7, 3-H), 8.39 (1H, dd, *J* 7.8 and 1.8, 4-H) and 9.03 (1H, dd, *J* 4.7 and 1.8, 2-H), (lit., ref.[69]); δ_C(75 MHz; $CDCl_3$) 16.7 (CH_3), 127.5, 129.1, 134.3, 135.0, 147.8, 149.1, 154.5, 183.7 (C=O) and 184.2 (C=O); *m*/*z* (ESI$^+$) 173.9 ([M + H]$^+$).

7-Methylquinoline-5,8-dione 3

To a solution of 2-bromo-6-methyl-1,4-benzoquinone[48,49] (101 mg, 0.5 mmol) in toluene (2 mL) was added acrolein dimethylhydrazone[45] (0.223 g, 2.27 mmol, 1 equiv.). The reaction mixture was heated at 80 °C for 4 h and after cooling and evaporation of the volatiles, the crude brown residue (130 mg) was purified by chromatography on silica gel (ether with gradient of ethanol) to afford **3** (6 mg, 7%); mp 131 °C (dec.) (lit.,[40] 175–80 °C); δ_H(300 MHz; $CDCl_3$) 2.23 (3H, d, *J* 1.5, CH_3), 7.01 (1H, m, 6-H), 7.67 (1H, dd, *J* 7.9 and 4.7, 3-H), 8.44 (1H, dd, *J* 7.9 and 1.7, 4-H) and 9.02 (1H, dd, *J* 4.7 and 1.7, 2-H); δ_C(75 MHz; $CDCl_3$) 16.3 (CH_3), 127.5, 129.5, 134.6, 136.1, 147.8 (2×), 154.5, 183.3 (C=O) and 185.0 (C=O); *m*/*z* (ESI$^+$) 173.9 ([M + H]$^+$).

6,7-Dimethylquinoline-5,8-dione 4

To a solution of 2-bromo-6,7-dimethyl-1,4-benzoquinone[50] (0.109 g, 0.51 mmol, 1 equiv.) in toluene (1 mL) heated at 80 °C was added dropwise a 1 M solution of acrolein dimethylhydrazone[45] in toluene (1.48 mL, 1.52 mmol, 3 equiv.). After 15 h heating, 0.45 mL of the latter solution (0.46 mmol, 0.9 equiv.) was added again, and the reaction was stopped after a further 18 h stirring, at which stage no starting material remained. The volatiles were then removed under reduced pressure and column chromatography on silica gel (Et_2O) yielded **4** (0.039 g, 41%); mp 152 °C ($CHCl_3$–pentane) (lit.,[42] 165–7 °C); (Found: C, 70.88; H, 4.85; N, 7.55. Calc. for $C_{11}H_9NO_2$: C, 70.58; H, 4.85; N, 7.49%); ν_{max}(neat)/cm^{-1} 3005 (CH_3), 1667 (C=O), 1616 (C=O) and 1578 (C=C); δ_H(400 MHz; $CDCl_3$) 2.14 and 2.18 (6H, s (×2), CH_3), 7.58 (1H, dd, *J* 8.0 and 4.5, 3-H), 8.33 (1H, dd, *J* 8.0 and 1.5, 4-H) and 8.92 (1H, dd, *J* 4.5 and 1.5, 2-H); δ_C(75 MHz; $CDCl_3$) 12.7 (CH_3), 13.0 (CH_3), 127.2, 128.8, 134.2, 142.9, 144.4, 147.5, 154.1, 183.1(C=O) and 184.1(C=O); *m*/*z* (DCI$^+$) 189.4 ([M + H]$^+$).

1,2-Diamino-3,6-dimethoxybenzene 7

To a solution of **10** (3.372 g, 17.03 mmol, 1 equiv.) in EtOAc (60 mL) was added palladium (10%/C, 0.36 g) and the mixture was stirred under hydrogen at atmospheric pressure for 5 h. After filtration on Celite and evaporation of the volatiles, **7** was obtained as a cream-coloured solid (2.782 g, 16.56 mmol, 97%), which was used directly in the next step (for prolonged storage, it is advisable to keep it under argon); mp 68–9 °C (lit.,[70] 68–70 °C); (Found: C, 57.24; H, 7.12; N, 16.79. Calc. for $C_8H_{12}N_2O_2$: C, 57.13; H, 7.20; N, 16.66%); ν_{max}(neat)/cm^{-1} 3423, 3403 and 3391 (NH_2), 2830 (OCH_3), 1634 (N–H) and 1487 (C=C); δ_H(300 MHz; $CDCl_3$) 3.50 (4H, br s, NH_2) 3.81 (6H, s, OCH_3) and 6.31 (2H, s, 4-H/5-H); δ_C(75 MHz; $CDCl_3$) 56.0 (OCH_3), 100.8 (CH), 124.6 (C_{quat}) and 143.2 (C_{quat}); *m*/*z* (ESI$^+$) 168.9 ([M + H]$^+$).

3,6-Dimethoxy-2-nitroaniline 10

Palladium (10%/C, 0.53 g) was added to a 9 : 1 mixture[53] of 1,4-dimethoxy-2,3-dinitro-benzene and its 2,5-dinitro isomer (5.00 g, 21.90 mmol) dissolved in EtOAc (100 mL). After stirring under hydrogen at atmospheric pressure—the course of the reaction being followed by tlc (R_f 0.71, CH_2Cl_2, orange spot)—the mixture was filtered on Celite; after evaporation of the volatiles, chromatography of the dark red residue on silica gel (pentane–ethyl acetate 4 : 1 to 1 : 1) gave **10** (3.372 g, 78%); mp 67–8 °C; ν_{max}(neat)/cm^{-1} 3495 and 3451 (NH_2), 2841 (OCH_3), 1621 (C=C), 1595 (NH), 1518 (C=C), 1472 (C=C) and 1344 (NO_2); δ_H(300 MHz; $CDCl_3$) 6.74 (1H, d, *J* 8.9, 5-H), 6.16 (1H, d, *J* 8.9, 4-H), 5.35 (2H, br s, NH_2) and 3.82 (6 H, s (2×), CH_3), (lit., ref.[57]); δ_C(75 MHz; $CDCl_3$) 56.4 (OCH_3), 56.6 (OCH_3), 98.2, 112.6, 127.4, 135.1, 141.5 and 148.5; *m*/*z* (ESI$^+$) 198.9 ([M + H]$^+$).

Quinoxaline-5,8-dione 5

To a solution of **7** (0.199 g, 1.18 mmol) in ethanol (5 mL) was added glyoxal trimer dihydrate (0.092 g, 0.44 mmol, 0.37 equiv.) and the mixture was heated at reflux temperature for 30 min. The solvent was removed under reduced pressure to afford 5,8-dimethoxyquinoxaline (0.239 g); ν_{max}(neat)/cm^{-1} 2837 (OCH_3), 1605 (C=C) and 1484 (C=C); δ_H(300 MHz; $CDCl_3$) 4.06 (6H, s, OCH_3), 6.97 (2H, s, 6-H/7-H) and 8.83 (2H, s, 2-H/3-H) (lit., ref.[71]); δ_C(75 MHz; $CDCl_3$) 56.2 (OCH_3), 107.5, 135.6, 143.9 and 148.8; *m*/*z* (DCI$^+$) 191.2 ([M + H]$^+$). To this quinoxaline (0.223 g, 1.17 mmol) dissolved in (1 : 1) acetonitrile–water (5 mL) was added portionwise a suspension of ceric ammonium nitrate (1.606 g, 2.99 mmol, 2.5 equiv.) in (20 : 1) acetonitrile–water (11 mL). The mixture was stirred at room temperature for 20 minutes, poured into ice-water (20 mL) and extracted with CH_2Cl_2 (3 × 20 mL). The organic layer was washed with water (20 mL), dried ($MgSO_4$) and volatiles were removed under reduced pressure to afford **5** as an orange solid (0.132 g, 70%), which was recrystallized twice from CH_2Cl_2–Et_2O for analytical purposes; mp 145–8 °C (dec.) (lit.,[58] 155–60 °C); (Found C, 59.78; H, 2.55; N, 17.27. Calc. for $C_8H_4N_2O_2$: C, 60.01; H, 2.52; N, 17.50%); λ_{max} (EtOH/nm) 275.0, 249.9, 215.0 (lit.[62]); ν_{max}(neat)/cm^{-1} 1671 (C=O); δ_H(300 MHz; $CDCl_3$) 7.25 (2H, s, 6-H/7-H) and 9.05 (2H, s, 2-H/3-H), (lit., ref.[52]); δ_C(75 MHz; $CDCl_3$) 138.7 (CH), 143.7 (C_{quat}), 149.0 (CH) and 182.5 (C=O); *m*/*z* (DCI$^+$) 161.3 ([M + H]$^+$).

2,3-Dimethylquinoxaline-5,8-dione 6

To a solution of **7** (1.00 g, 5.96 mmol) in ethanol (25 mL) was added freshly distilled 2,3-butanedione (0.6 mL, 6.84 mmol, 1.15 equiv.) and the mixture was heated at reflux temperature for 30 min. The volatiles were removed under reduced pressure which afforded 5,8-dimethoxy-2,3-dimethylquinoxaline (1.224 g, 94%) as a flocculent yellow solid; mp 168–9 °C (lit.,[62] 171–2 °C); (Found C, 65.64;

H, 6.54; N, 12.55. Calc. for $C_{12}H_{14}N_2O_2$: C, 66.04, H, 6.47; N, 12.84%); ν_{max}(neat)/cm^{-1} 3001 (CH_3), 2734 (OCH_3), 1609 (C=C) and 1488 (C=C); δ_H(300 MHz; $CDCl_3$) 2.69 (6H, s, CH_3), 3.95 (6H, s, OCH_3), 6.83 (2H, s, 6-H/7-H); δ_C(75 MHz; $CDCl_3$) 23.1 (C-CH_3), 56.0 (OCH_3), 106.2, 133.5, 148.2, 152.5; *m/z* (DCI^+) 219.5 ($[M + H]^+$). To this quinoxaline (0.249 g, 1.14 mmol) stirred in (1 : 1) acetonitrile–water (5 mL) was added portionwise a suspension of ceric ammonium nitrate (1.574 g, 2.87 mmol, 2.5 equiv.) in (20 : 1) acetonitrile–water (11 mL). The mixture was stirred at room temperature for 20 minutes, poured into ice-water (20 mL) and extracted with CH_2Cl_2 (3 × 20 mL). The organic layer was washed with water (20 mL), dried ($MgSO_4$) and volatiles were removed under reduced pressure to afford **6** (0.203 g, 94%) as a yellow solid, which was recrystallized twice from CH_2Cl_2–Et_2O for analytical purposes; mp 174–5 °C (dec.) (lit.,[72] 176–8 °C); (Found: C, 63.96; H, 4.70; N, 14.50. Calc. for $C_{10}H_8N_2O_2$: C, 63.83; H, 4.29; N, 14.89%); λ_{max} (EtOH/nm) 290.0, 255.0, 230.0 (lit.[62]); ν_{max}(neat)/cm^{-1} 1671 (C=O); δ_H(300 MHz; $CDCl_3$) 2.79 (6H, s, OCH_3) and 7.13 (2H, s, 6-H/7-H); δ_C(75 MHz; $CDCl_3$) 23.0 (2-CH_3/3-CH_3), 138.2 (6-C/7-C), 141.1(C_{quat}), 159.0 (C_{quat}) and 183.4 (C=O); *m/z* (DCI^+) 189.4 ($[M + H]^+$).

Cyclic voltammetry

Electrochemical measurements were performed using a conventional three electrodes system (660B model potentiostat, CH-Instruments). Automatic iR compensation was performed before each cyclic voltammetry experiment. The working glassy carbon disc electrode (3 mm diameter, from CH-Instruments) was polished with 2 μm diamond paste before use. Electrode potentials were referred to the standard calomel electrode (SCE) potential in aqueous media. 1,1′-Dimethyl-4,4′-bipyridinium dichloride (methyl viologen, denoted MV^{2+}) was also used as an internal reference in aqueous electrolyte. Solutions were degassed with N_2 before each measurement. All experiments were run at 20 °C. Tetra-*n*-butylammonium perchlorate (TBAP, Fluka puriss) was dried under vacuum at 80 °C for 3 days. Distilled water was obtained from an Elgastat water purification system (5 MΩ cm). Other reagent grade chemicals were used without further purification.

Enzyme preparation

Plasmodium falciparum TrxR and Trx were prepared as described.[73] Both *P. falciparum* GR[17] and human GR[74] were respectively produced as described and kindly provided by Prof. Heiner Schirmer, Center for Biochemistry, Heidelberg University. The enzyme stock solutions used for the kinetic determinations were pure as judged from a silver-stained SDS-PAGE and had specific activity of 21 U mg^{-1} in Trx reduction assay for PfTrxR, 143 U mg^{-1} and 168 U mg^{-1} in GSSG reduction assay for PfGR and hGR, respectively.

Enzyme assays

All kinetic studies were carried out at 25 °C in a volume of 1 mL in the presence of 100 μM NADPH. The glutathione reductase assay mixtures contained 47 mM potassium phosphate buffer pH 6.9, 200 mM KCl and 1 mM EDTA. The thioredoxin reductase assay mixtures contained 100 mM potassium phosphate buffer pH 7.4 and 2 mM EDTA. Inhibitor stock solutions were prepared in 100% DMSO. A 1% final DMSO concentration was kept constant in the assay cuvette.

IC_{50} determinations

The standard glutathione reductase and thioredoxin reductase assay mixtures contained 1 mM GSSG or 26 μM Trx, as the disulfide substrate, respectively. In the TrxR assay, 1 mM GSSG was added to recycle continuously Trx from $Trx(SH)_2$. The reaction was started with the addition of the enzyme (GR: 10 mU or 1.1 nM final in the cuvette; TrxR: 10 mU or 7.7 nM final in the cuvette) and initial rates were determined from NADPH oxidation measured at 340 nm (ε_{340}: 6.22 mM^{-1} cm^{-1}) at 25 °C. IC_{50} values were evaluated in duplicate in the presence of ten inhibitor concentrations ranging from 0 to 200 μM.

Evaluation of inhibition type and K_i under steady-state conditions

Types of inhibition and inhibition constants for **1**,**4-NQ** and **6** were determined in duplicate experiments. *P. falciparum* TrxR activity was measured at different concentrations of **1**,**4-NQ** (0–2.5 μM) or of inhibitor **6** (0–1 μM) in the presence of varying concentrations of Trx (6–244 μM) at a constant NADPH concentration of 100 μM in the presence of 1 mM GSSG. K_m and V_{max} values were determined by fitting data to the Michaelis–Menten equation using nonlinear regression analysis.[75] Inhibition of GSSG reduction by quinones was measured as a function of substrate concentration, and the experimental data were fitted by using nonlinear regression analysis software (Kaleidagraph) to eqn (1) for competitive inhibition, where [S] is the concentration of the variable substrate, [I] is the inhibitor concentration, V_{max} is the maximal rate, K_m is the Michaelis–Menten constant, and K_i is the inhibition constant for I binding to the ES complex.

$$v = \frac{V_{max} \cdot [S]}{K_m \cdot (1 + \frac{[I]}{K_i}) + [S]} \quad (1)$$

Quinone reductase activity

The ability of the glutathione reductase or the thioredoxin reductase to reduce the naphthoquinone was assayed at 25 °C by monitoring the oxidation of 100 μM NADPH at 340 nm. The assays, in a total volume of 1 mL, contained the GR- or TrxR-buffer and the enzyme (PfGR: 118 pmol to 1.18 nmol; hGR: 458 pmol to 1.14 nmol; PfTrxR: 15.4 pmol to 154 pmol per assay). The naphthoquinone was dissolved in DMSO and the NADPH-oxidase activity was measured at four to five different 1,4-NQ concentrations in duplicate (10–400 μM) in the presence of 1% DMSO. For the determination of K_m and V_{max} values, the steady-state rates were graphically fitted by using nonlinear regression analysis software (Kaleidagraph) to the Michaelis–Menten equation, and the turnover number k_{cat} and the catalytic efficiency k_{cat}/K_m were calculated.

Time-dependent inactivation

For determining the time-dependent inactivation of *P. falciparum* TrxR, the residual TrxR activity was monitored over time (0.25, 5, 10, and 15, min-incubation periods) by following an incubation

protocol.[76] All reaction mixtures (final volume of 200 μL) contained 160 μM NADPH, varying inhibitor concentrations, *P. falciparum* TrxR (1.23 nmol), 2% DMSO in TrxR buffer at 25 °C. Inhibitor concentrations used were 0–0.5–1.0–2.0–5.0 μM for **1**,**4-NQ** and 0–0.5–1.0–2.0–3.0–4.0–5.0–20.0 μM for aza-naphthoquinone **5**. At different time points, 5 μL-aliquots of each reaction mixture were removed and the residual activity was measured in the standard Trx reduction assay at 25 °C (in the presence of 24 μM Trx, 1 mM GSSG and 100 μM NADPH). 2% DMSO was used in control assays. From semi-logarithmic plots $\ln(v_i/v_0)$ *versus* incubation time apparent rate constants of irreversible inhibition (k_{obs}) of the fraction of non-inhibited enzyme activity *versus* [I] were fitted to eqn (2):

$$k_{obs} = \frac{k_i \cdot [\mathrm{I}]}{K_\mathrm{I} + [\mathrm{I}]} \quad (2)$$

where K_I represents the dissociation constant of the inhibitor, and k_i is the first order rate constant for irreversible inactivation, respectively.

Acknowledgements

Our work is supported by the Centre National de la Recherche Scientifique (E.D.C.) and by the Deutsche Forschungsgemeinschaft *via* the SFB 544 "Control of Tropical Infectious Diseases," project B14 (E.D.C.) and the grant BE1540/4-4 (K.B.). T.B. is grateful to the French "Ministère de l'Éducation Nationale, de la Recherche et de la Technologie" for a doctoral fellowship.

References

1 I. W. Sherman, in *Molecular Approaches to Malaria*, American Society of Microbiology Press, Riverside, California, US, 2005.
2 J. G. Breman, M. S. Alilio and A. Mills, *Am. J. Trop. Med. Hyg.*, 2004, **71**, 1–15.
3 K. Maitland, M. Makanga and T. N. Williams, *Curr. Opin. Infect. Dis.*, 2004, **17**, 405–412.
4 L. B. Stewart, W. Peters and B. L. Robinson, *Ann. Trop. Med. Parasitol.*, 2004, **98**, 763–783.
5 M. Schlitzer, *ChemMedChem*, 2007, **2**, 944–986.
6 K. Becker, L. Tilley, J. L. Vennerstrom, D. Roberts, S. Rogerson and H. Ginsburg, *Int. J. Parasitol.*, 2004, **34**, 163–189.
7 R. L. Krauth-Siegel, H. Bauer and R. H. Schirmer, *Angew. Chem., Int. Ed.*, 2005, **44**, 690–715.
8 S. Rahlfs and K. Becker, *Mini-Rev. Med. Chem.*, 2006, **6**, 163–176.
9 K. Becker, S. Rahlfs, C. Nickel and R. H. Schirmer, *Biol. Chem.*, 2003, **384**, 551–566.
10 S. Müller, *Mol. Microbiol.*, 2004, **53**, 1291–1305.
11 Y. Zhang, I. König and R. H. Schirmer, *Biochem. Pharmacol.*, 1988, **37**, 861–865.
12 Y. A. Zhang, E. Hempelmann and R. H. Schirmer, *Biochem. Pharmacol.*, 1988, **37**, 855–860.
13 M. Cappadoro, G. Giribaldi, E. O'Brien, F. Turrini, F. Mannu, D. Ulliers, G. Simula, L. Luzzatto and P. Arese, *Blood*, 1998, **92**, 2527–2534.
14 E. Davioud-Charvet, S. Delarue, C. Biot, B. Schwöbel, C. C. Böhme, A. Müssigbrodt, L. Maes, C. Sergheraert, P. Grellier, R. H. Schirmer and K. Becker, *J. Med. Chem.*, 2001, **44**, 4268–4276.
15 C. Biot, H. Bauer, R. H. Schirmer and E. Davioud-Charvet, *J. Med. Chem.*, 2004, **47**, 5972–5983.
16 H. Bauer, K. Fritz-Wolf, A. Winzer, S. Kuhner, S. Little, V. Yardley, H. Vezin, B. Palfey, R. H. Schirmer and E. Davioud-Charvet, *J. Am. Chem. Soc.*, 2006, **128**, 10784–10794.
17 P. M. Färber, L. D. Arscott, C. H. Williams, Jr., K. Becker and R. H. Schirmer, *FEBS Lett.*, 1998, **422**, 311–314.
18 R. M. Luond, J. H. McKie, K. T. Douglas, M. J. Dascombe and J. Vale, *J. Enzyme Inhib.*, 1998, **13**, 327–345.
19 P. Grellier, J. Sarlauskas, Z. Anusevicius, A. Maroziene, C. Houee-Levin, J. Schrevel and N. Cenas, *Arch. Biochem. Biophys.*, 2001, **393**, 199–206.
20 M. Wainwright and L. Amaral, *Trop. Med. Int. Health*, 2005, **10**, 501–511.
21 R. H. Schirmer, J. G. Müller and R. L. Krauth-Siegel, *Angew. Chem., Int. Ed. Engl.*, 1995, **107**, 153–157.
22 C. Nickel, S. Rahlfs, M. Deponte, S. Koncarevic and K. Becker, *Antioxid. Redox Signaling*, 2006, **8**, 1227–1239.
23 Z. Krnajski, T. W. Gilberger, R. D. Walter, A. F. Cowman and S. Muller, *J. Biol. Chem.*, 2002, **277**, 25970–25975.
24 C. H. Williams, L. D. Arscott, S. Muller, B. W. Lennon, M. L. Ludwig, P. F. Wang, D. M. Veine, K. Becker and R. H. Schirmer, *Eur. J. Biochem.*, 2000, **267**, 6110–6117.
25 P. J. McMillan, L. D. Arscott, D. P. Ballou, K. Becker, C. H. Williams, Jr. and S. Muller, *J. Biol. Chem.*, 2006, **281**, 32967–32977.
26 S. Gromer, S. Urig and K. Becker, *Med. Res. Rev.*, 2004, **24**, 40–89.
27 E. Davioud-Charvet, M. J. McLeish, D. M. Veine, D. Giegel, L. D. Arscott, A. D. Andricopulo, K. Becker, S. Muller, R. H. Schirmer, C. H. Williams, Jr. and G. L. Kenyon, *Biochemistry*, 2003, **42**, 13319–13330.
28 B. Lee, H. Bauer, J. Melchers, T. Ruppert, L. Rattray, V. Yardley, E. Davioud-Charvet and R. L. Krauth-Siegel, *J. Med. Chem.*, 2005, **48**, 7400–7410.
29 A. D. Andricopulo, M. B. Akoachere, R. Krogh, C. Nickel, M. J. McLeish, G. L. Kenyon, L. D. Arscott, C. H. Williams, Jr., E. Davioud-Charvet and K. Becker, *Bioorg. Med. Chem. Lett.*, 2006, **16**, 2283–2292.
30 J. J. Kessl, N. V. Moskalev, G. W. Gribble, M. Nasr, S. R. Meshnick and B. L. Trumpower, *Biochim. Biophys. Acta*, 2007, **1767**, 319–326.
31 K. Lopez-Shirley, F. Zhang, D. Gosser, M. Scott and S. R. Meshnick, *J. Lab. Clin. Med.*, 1994, **123**, 126–130.
32 Y. P. Wan, T. H. Porter and K. Folkers, *Proc. Natl. Acad. Sci. USA*, 1974, **71**, 952–956.
33 R. M. Luond, J. H. McKie and K. T. Douglas, *Biochem. Pharmacol.*, 1993, **45**, 2547–2549.
34 H. J. Teuber and N. Götz, *Chem. Ber.*, 1954, **87**, 1236–1251.
35 D. W. Cameron, K. R. Deutscher and G. I. Feutrill, *Aust. J. Chem.*, 1982, **35**, 1439–1450.
36 A. S. Amarasekara, *Synth. Commun.*, 1999, **29**, 3063–3066.
37 J. Cossy and D. Belotti, *Tetrahedron Lett.*, 2001, **42**, 4329–4331.
38 R. Barret and M. Daudon, *Tetrahedron Lett.*, 1990, **34**, 4871–4872.
39 W. G. Christiansen and M. A. Dolliver, *J. Am. Chem. Soc.*, 1941, **63**, 1470.
40 R. Long and K. Schofield, *J. Chem. Soc.*, 1953, 3161–3167.
41 V. Petrow and B. Sturgeon, *J. Chem. Soc.*, 1954, 570–574.
42 A. J. Lin, B. J. Lillis and A. C. Sartorelli, *J. Med. Chem.*, 1975, **18**, 917–921.
43 B. Serckx-Poncin, A.-M. Hesbain-Frique and L. Ghosez, *Tetrahedron Lett.*, 1982, **23**, 3261–3264.
44 J. M. Perez, C. Avendano and J. C. Menendez, *Tetrahedron*, 1995, **51**, 6573–6586.
45 E. Gomez-Bengoa and A. M. Echavarren, *J. Org. Chem.*, 1991, **56**, 3497–3501.
46 K. J. M. Andrews, D. H. Marrian and D. R. Maxwell, *J. Chem. Soc.*, 1956, 1844–1854.
47 A. Tomatsu, S. Takemura, K. Hishimoto and M. Nakata, *Synlett*, 1999, 1474–1476.
48 L. Gu, C. Liu, J. Xu and E. K. Tsoo, *Tetrahedron*, 1990, **46**, 3199–3210.
49 W. S. Murphy and M. Bertrand, *J. Chem. Soc., Perkin Trans. 1*, 1998, 4115–4120.
50 E. G. Kleinschmidt and H. Brauniger, *Pharmazie*, 1969, **24**, 94–95.
51 A. Taleb, F. Alvarez, P. Nebois and N. Walchshofer, *Heterocycl. Commun.*, 2006, **12**, 111–114.
52 Y. Kitahara, S. Nakahara, Y. Tanaka and A. Kubo, *Heterocycles*, 1992, **34**, 1623–1630.
53 C. Lion, R. Baudry, M. Hedayatullah, L. Da Conceicao, S. Genard and J. Maignan, *J. Heterocycl. Chem.*, 2002, **39**, 125–130.
54 P. Hammershoej, T. K. Reenberg, M. Pittelkow, C. B. Nielsen, O. Hammerich and J. B. Christensen, *Eur. J. Org. Chem.*, 2006, 2786–2794.
55 I. D. Entwistle, R. A. W. Johnstone and T. J. Povall, *J. Chem. Soc., Perkin Trans. 1*, 1975, 1300–1301.
56 D. L. Clive, A. G. Angoh and S. M. Bennett, *J. Org. Chem.*, 1987, **52**, 1339–1342.
57 C. W. Lai, C. K. Lam, H. K. Lee, T. C. Mak and H. N. Wong, *Org. Lett.*, 2003, **5**, 823–826.

58 C. W. Rees and D. E. West, *J. Chem. Soc. C*, 1970, 583–589.
59 H. Bock, P. Dickmann and H.-F. Herrmann, *Z. Naturforsch.*, 1991, **46b**, 326–338.
60 J. Q. Chambers, in *The chemistry of the quinonoid compounds*, ed. S. Patai, Wiley & Sons, London, New York, Sydney, Toronto, 1974, part 2, ch. 14, pp. 737–791.
61 D. H. Evans and D. A. Griffith, *J. Electroanal. Chem.*, 1982, **134**, 301–310.
62 W. F. Gum, Jr. and M. M. Joullié, *J. Org. Chem.*, 1967, **32**, 53–59.
63 J. J. Newsome, M. A. Colucci, M. Hassani, H. D. Beall and C. J. Moody, *Org. Biomol. Chem.*, 2007, **5**, 3665–3673.
64 M. A. Colucci, G. D. Couch and C. J. Moody, *Org. Biomol. Chem.*, 2008, **6**, 637–656.
65 N. Cenas, H. Nivinskas, Z. Anusevicius, J. Sarlauskas, F. Lederer and E. S. Arner, *J. Biol. Chem.*, 2004, **279**, 2583–2592.
66 R. Kitz and I. B. Wilson, *J. Biol. Chem.*, 1962, **237**, 3245–3249.
67 J. S. Lazo, D. C. Aslan, E. C. Southwick, K. A. Cooley, A. P. Ducruet, B. Joo, A. Vogt and P. Wipf, *J. Med. Chem.*, 2001, **44**, 4042–4049.
68 A. Haber and B. D. Hilton, *Org. Magn. Reson.*, 1983, **21**, 168–172.
69 J. M. Wagner, C. J. McElhinny, Jr., A. H. Lewin and F. I. Carroll, *Tetrahedron: Asymmetry*, 2003, **14**, 2119–2125.
70 I. A. Shaikh, F. Johnson and A. P. Grollman, *J. Med. Chem.*, 1986, **29**, 1329–1340.
71 I. Baxter, D. W. Cameron and R. B. Titman, *J. Chem. Soc. C*, 1971, 1253–1256.
72 B. Venugopalan, C. P. Bapat, P. J. Karnik and N. J. De Souza, *Indian J. Chem.*, 1990, **29B**, 364–365.
73 S. M. Kanzok, R. H. Schirmer, I. Türbachova, R. Iozef and K. Becker, *J. Biol. Chem.*, 2000, **275**, 40180–40186.
74 A. Nordhoff, U. S. Bücheler, D. Werner and R. H. Schirmer, *Biochemistry*, 1993, **32**, 4060–4066.
75 I. H. Segel, in *Enzyme Kinetics. Behavior and analysis of rapid equilibrium and steady-state enzyme systems*, John Wiley and Sons, New York, 1975.
76 S. Gromer, H. Merkle, R. H. Schirmer and K. Becker, *Methods Enzymol.*, 2002, **347**, 382–394.

